

Laser pulse annealing of ion-implanted GaAs

S. U. Campisano, G. Foti, and E. Rimini

Istituto di Struttura della Materia, dell' Universita-CorsoItalia 57, 195129 Catania, Italy

F. H. Eisen

Rockwell International Science Center, Thousand Oaks, California 91360

W. F. Tseng,^{a)} M-A. Nicolet, and J. L. Tandon^{b)}

California Institute of Technology, Pasadena, California 91125

(Received 11 May 1979; accepted for publication 25 July 1979)

GaAs single-crystals wafers are implanted at room temperature with 400-keV Te^+ ions to a dose of $1 \times 10^{15} \text{ cm}^{-2}$ to form an amorphous surface layer. The recrystallization of this layer is investigated by backscattering spectrometry and transmission electron microscopy after transient annealing by Q -switched ruby laser irradiation. An energy density threshold of about 1.0 J/cm^2 exists above which the layer regrows epitaxially. Below the threshold the layer is polycrystalline; the grain size increases as the energy density approaches threshold. The results are analogous to those reported for the elemental semiconductors, Si and Ge. The threshold value observed is in good agreement with that predicted by the simple model successfully applied previously to Si and Ge.

PACS numbers: 61.70.Im, 79.20.Ds, 81.40.Ef

INTRODUCTION

A great effort was made in the last few years to understand the interaction of a laser beam with ion-implanted semiconductors as a new method to anneal damage.¹ The material most studied so far is elemental silicon and a clear picture has emerged from these investigations: There is a threshold in the energy density of the laser pulse above which the damaged Si layer liquifies and then regrows epitaxially.²⁻⁴ Below threshold, the layer turns polycrystalline and the grain size depends on the energy density of the pulse.⁵

The concept of pulse annealing appears particularly advantageous in connection with compound semiconductors such as GaAs. Steady-state (thermal) annealing of ion-implanted layers of GaAs requires particular precautions, such as controlled ambients or capping, to prevent the dissociation of the compound at the high annealing temperatures involved.⁶ Recent results indicate that pulsed annealing of ion-implanted GaAs layers in air, without capping, may offer an attractive alternative to furnace annealing.⁷⁻¹⁰

The present study was therefore initiated to investigate in some detail the crystallinity of ion-implanted GaAs layers after pulse laser irradiation of variable energy density.

EXPERIMENTAL PROCEDURE

Semi-insulating GaAs wafers of $\langle 100 \rangle$ orientation were implanted at room temperature with 400-keV Te to a fluence of about $1 \times 10^{15} \text{ cm}^{-2}$. This implantation produces an amorphous layer of about 2300 Å thickness. To minimize channeling, the ion beam was oriented at an angle of $\sim 10^\circ$ against the normal to the wafer surface.

Laser irradiation was performed in air by a Q -switched

ruby pulse ($\lambda = 0.694 \mu\text{m}$) of 15 and 50 ns (FWHM) duration, respectively. The spot diameter ranged from 1 to 10 cm. The incident energy density varied from 0.2 to 2.0 J/cm^2 . Channeling and backscattering spectrometry measurements were performed with 2.5-MeV $^4\text{He}^+$ to investigate the thickness of the damaged layer and its recovery after laser irradiation. Information on the microstructure of the layer after laser irradiation was obtained by transmission electron microscopy.

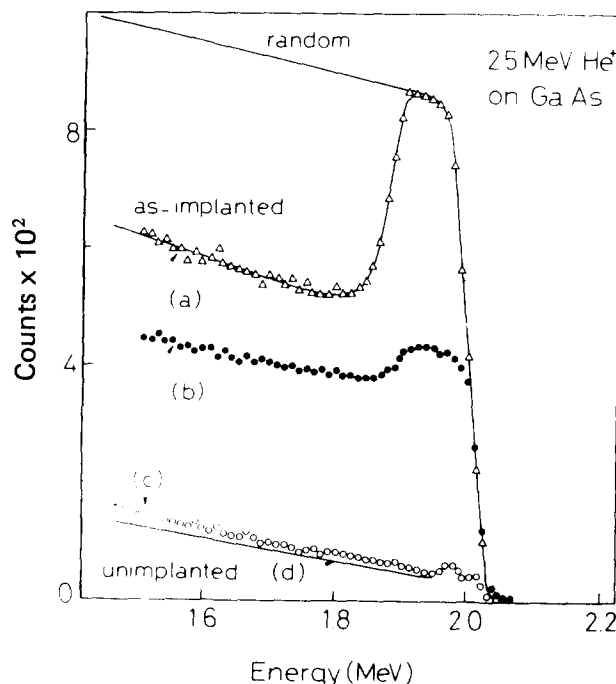


FIG. 1. Backscattering spectra of 2.5-MeV $^4\text{He}^+$ ions incident in a random direction in the $\langle 100 \rangle$ direction of GaAs samples implanted with 400-KeV $\text{Te} 10^{15} \text{ cm}^{-2}$, after laser irradiation of energy (a) 0.2 to 0.8 J/cm^2 , (b) 0.9 J/cm^2 , (c) $1.0\text{--}1.4 \text{ J/cm}^2$. Curve (d) is obtained from the unimplanted $\langle 100 \rangle$ GaAs sample.

^{a)}Present address: Electronic Technology Division, Naval Research Laboratory, Washington, D.C. 20375.

^{b)}Present address: Rockwell International Science Center, Thousand Oaks, Calif. 91360.

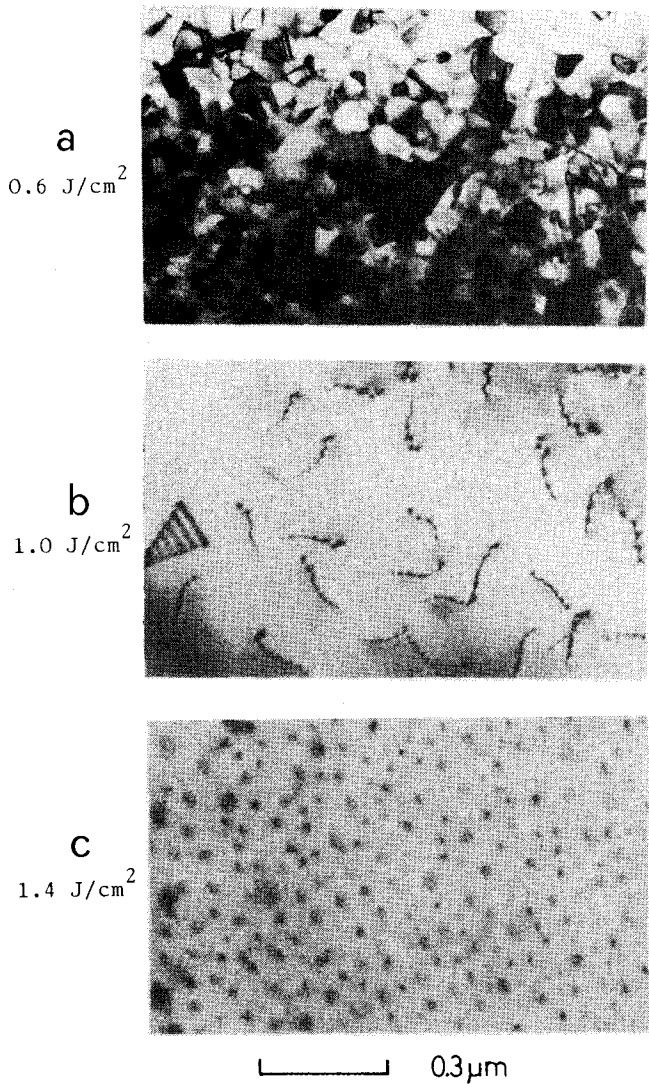


FIG. 2. TEM micrographs of GaAs implanted with 400-keV Te^+ (10^{15} cm^{-2}) and irradiated with 50 nsec ruby laser of (a) 0.6 J/cm^2 , (b) 1.0 J/cm^2 , (c) 1.4 J/cm^2 .

RESULTS

Channeling effect measurements indicate that the recovery of the implanted amorphous layer exhibits a threshold with laser beam energy density. This threshold has a value of about 1.0 J/cm^2 . Above that threshold value, the backscattering yield observed with $\langle 100 \rangle$ aligned incidence of the He beam becomes comparable to that measured on an unimplanted single-crystal wafer, as shown in Fig. 1. A backscattering spectrum taken at random incidence of the He beam shows that the Te implantation destroys the monocrystalline structure of the wafer over a depth of approximately 2300 \AA . This layer is amorphous in structure as was determined by electron diffraction measurements. A ruby laser pulse of 1 J/cm^2 thus transforms the implanted amorphous layer into an epitaxial layer with good crystalline quality. For energy densities below 0.8 J/cm^2 , the backscattering yield of a laser-irradiated sample is the same as that of an unirradiated one. Near threshold, at 0.9 J/cm^2 , the yield observed with aligned He beam incidence decreases only by

about 50%. No movement of the original amorphous-to-crystal interface is detected. In the range of $1.0\text{--}1.4 \text{ J/cm}^2$ beyond threshold, channeling effect gives the same spectrum, and this spectrum differs little from that of an unimplanted wafer. In particular, the As and Ga signals for backscattering from the surfaces of the unimplanted and the regrown sample are indistinguishable. This suggests that within the accuracy of our measurement, the stoichiometry of the regrown layer is preserved. It has been shown previously⁸ that ion-implanted GaAs layers regrown by pulsed ruby irradiation maintain stoichiometry to better than 1%. After Nd-YAG irradiation of GaAs-Te-implanted samples, an excess of Ga on the surface has been reported.¹¹

Transmission electron micrographs of samples irradiated with energy densities of $0.6, 1.0,$ and 1.4 J/cm^2 are shown in Figs. 2(a), 2(b) and 2(c), respectively. At 0.6 J/cm^2 , polycrystalline material is formed. At 1.0 J/cm^2 , single-crystalline material is formed with stacking faults and with dislocations whose density is about $3 \times 10^5 \text{ cm/cm}^2$. By counting the number of the dark fringes of the stacking faults, the thickness of the layer amounts to about 2500 \AA which corre-

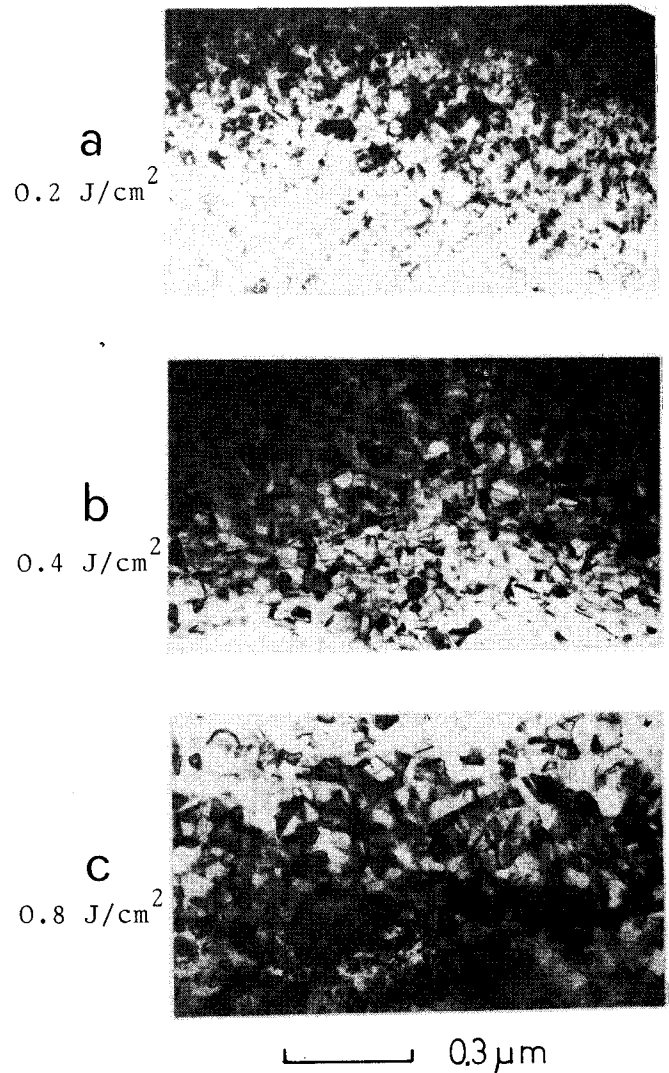


FIG. 3. TEM micrographs showing polycrystals in the Te-implanted GaAs after laser irradiation of (a) 0.2 J/cm^2 , (b) 0.4 J/cm^2 , and (c) 0.8 J/cm^2 .

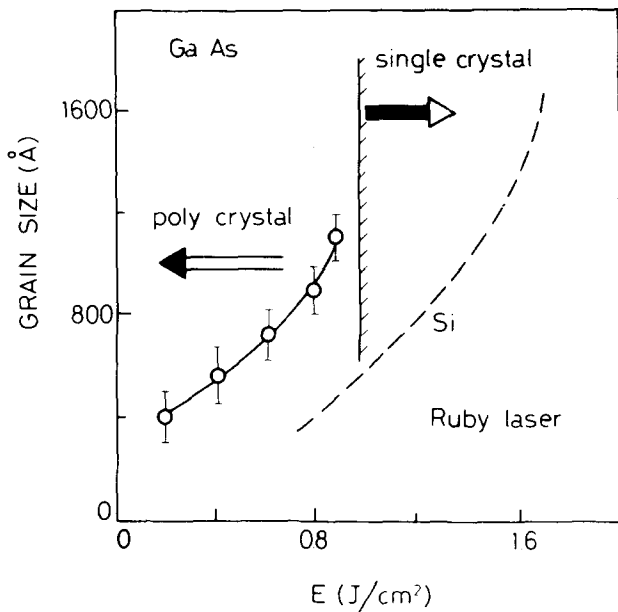


FIG. 4. Average grain size obtained from TEM micrographs of the polycrystalline GaAs layer formed by transient annealing with a ruby-laser pulse of varying energy density. Prior to the laser irradiation, the (100) GaAs substrate had been implanted with 400-keV Te at room temperature at a dose of $1 \times 10^{15} \text{ cm}^{-2}$. The bars represent the spread in the diameter of the grains. The dashed line is that given in Ref. 5, for ion-implanted Si and laser irradiation.

sponds to the initial thickness of the amorphous layer. At 1.4 J/cm^2 , single-crystalline material is formed with dispersed defects [black spots in Fig. 2(c)] of about $3 \times 10^{10}/\text{cm}^2$. These defects are less than 100 Å in size and located very near the surface, as was determined by stereomicrographs. The physical identity of these defects has yet to be established.

The difference in microstructure between Figs. 2(a) and 2(b) suggests the existence of a threshold energy density. Its value has been determined to be in the close vicinity of 1.0 J/cm^2 based on the sequence of micrographs shown in Fig. 3 for 0.2, 0.4, and 0.8 J/cm^2 ruby-laser energy density. At 0.9 J/cm^2 the layer is still polycrystalline (see Fig. 4).

We have also observed that the size of the grains in polycrystalline layers obtained after laser irradiation below threshold depends on the energy density of the ruby-laser pulse. From micrographs such as shown in Fig. 2(a) and Fig. 3, we have determined the average dimension of the grains in the polycrystalline layers. The average grain size increases with increasing energy density of the laser irradiation. The results are summarized in Fig. 4. The bars represent the spread in the distribution of the grain diameter. The average grain size ranges from 400 to 1100 Å on going from 0.2 to 0.9 J/cm^2 . Near threshold ($\sim 1.0 \text{ J/cm}^2$) the lateral nonuniformities of the ruby-laser spot becomes crucial in determining the structural configuration of the irradiated layer.

For comparison, the results previously reported for ruby-laser and ion-implanted amorphous Si layers are shown as a dashed line in Fig. 4. The two curves are similar, but grain sizes of irradiated GaAs layers are bigger for GaAs than for Si for the same energy density of the ruby laser. The difference may be due to the different thermal and optical properties of the two semiconductors.

DISCUSSION AND CONCLUSION

The existence of a threshold energy, separating films of polycrystalline and single-crystalline structure depending on the energy density of the laser irradiation as well as the dependence of grain size on energy density below threshold observed here for GaAs, are analogous to the results found with Si. We therefore interpret our results in the same fashion, as was initially proposed by Shtyrkov *et al.*¹² Above threshold, the energy deposited by the laser beam suffices to melt a layer of GaAs which exceeds the depth of the amorphous implanted layer. Below threshold, the molten zone never reaches the single-crystalline substrate and thus will not regrow epitaxially.

This simple model has previously been used in the literature to describe the interaction of a laser beam with ion-implanted silicon and germanium in terms of energy transfer from the laser beam to the semiconductor.¹³ The effect was described by the solution of the heat equation with a depth-dependent source term associated to the light absorption. The solution requires a numerical approach to include phase transitions and changes of optical and thermal parameters with temperature and structure, as detailed for the silicon case.¹⁴ We have applied the same method to the case of GaAs. The following values were used in the calculations: conductivity [8 W/cm K and 0.3 W/cm K at room temperature (RT) and at the melting point respectively;] reflectivity: 0.4 and 0.7 for solid and liquid phase; absorption coefficient: 10^5 cm^{-1} ; latent heat of fusion: 60 $\mu\text{J/g}$; and heat capacity: 35 J/g. The high value of the absorption coefficient in the amorphous material implies that a fraction of about 70% of the incident energy is absorbed in the first 1000 Å. The changes in α between the amorphous and the single-crystal substrate were then neglected. The results of the calculations are reported in Fig. 5, where the thickness of the molten GaAs region is plotted versus the incident energy density of

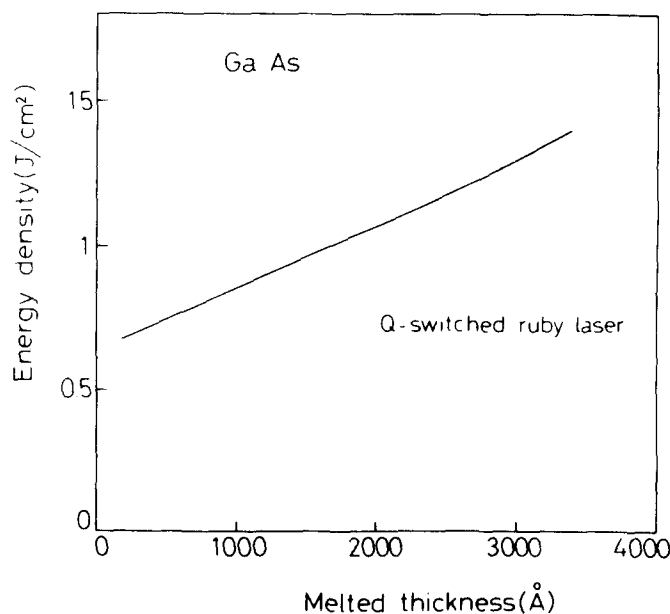


FIG. 5. Calculated energy density of Q-switched ruby laser single pulse versus melted thickness in amorphous GaAs lasers. The shape of the pulse has been assumed Gaussian with a FWHM of 50 ns.

the Q -switched ruby laser pulse of 50 ns duration. The transition to single crystal of a 2000-Å-thick amorphous layer occurs when the energy density of the pulse is at least enough to melt all this disordered region. The epigrowth on the underlying single crystal is then possible. The calculations reported in Fig. 5 predicts a value of 1.1 J/cm² agrees well with the experimental data of 1.0 J/cm².

We conclude from these results that the same simple model of pulse annealing by transient melting and subsequent regrowth applies equally to ion-implanted Si, Ge, and GaAs. The prediction, thus, is that our results are independent of the substrate orientation of the GaAs. In Si, the atomic specie used for the formation of the amorphous layer affects the result only to second order.¹⁵ The detailed structure of the density of states below and above the band edges could be of relevance mainly for light energy comparable with the band gap of the semiconductor. One would thus surmise that our results apply to GaAs regardless of the implanted specie as well. It is interesting to observe at this point that amorphous ion-implanted layers of Si (and Ge) differ from those of ion-implanted GaAs when the regrowth is induced in the solid phase at steady state, i.e., in a furnace substantially below the melting point ($\sim \frac{1}{2}T_{cm}$ in °K). The amorphous Si layer regrows in the $\langle 110 \rangle$ and $\langle 100 \rangle$ direction with little residual damage,¹⁶ but the amorphous GaAs layer regrown in the solid phase contains high amounts of residual damage in all major crystalline direction of regrowth.¹⁷ It has been shown that solid-phase regrowth of excellent quality can also be induced in Si by a scanned Ar laser beam.¹⁸ It would be of interest to see if GaAs behaves as Si in this mode of transient solid-state regrowth or not. First experiments of this kind have recently been reported, but details of the regrowth have not been investigated.¹⁹

ACKNOWLEDGMENTS

The authors are indebted to P. Baeri for providing the calculations reported in Fig.5. At Cal Tech, this work was supported financially in part by the Office of Naval Research (L.R. Copper); at the Rockwell International Science Center by the Defense Advanced Research Projects Agency under

ARPA Order No. 3595, Contract No. MDA 903-78-C-0285; at Catania by GNSM-CNR. This help is gratefully acknowledged.

¹See, for example, "Laser Effects in Ion Implanted Semiconductors", edited by E. Rimini (unpublished); "Laser-Solid Interactions and Laser Processing", edited by S.D. Ferris, H.J. Leamy, and J.M. Poate (AIP, New York, 1979).

²I.B. Khaibullin, E.I. Shtyrkov, M.M. Zaripov, R.M. Baryazitov, and M.F. Galjautdinov, *Radiat. Eff.* **36**, 225 (1978).

³G. Foti, E. Rimini, M. Bertolotti, and G. Vitali, *Phys. Lett.* **65** A, 431 (1978).

⁴D.H. Auston, C.M. Surko, T.N.C. Venkatesan, R.E. Slusher, and J.A. Galovchenko, *Appl. Phys. Lett.* **33**, 437 (1978).

⁵W.F. Tseng, J.W. Mayer, S.U. Campisano, G. Foti, and E. Rimini, *Appl. Phys. Lett.* **32**, 824 (1978).

⁶K. Gamo, I. Inada, S. Krekeler, J.W. Mayer, F.H. Eisen, and B.M. Welch, *Solid-State Electron.* **20**, 213 (1977).

⁷J.A. Golovchenko and T.N.C. Venkatesan, *Appl. Phys. Lett.* **32**, 147 (1978).

⁸S.U. Campisano, I. Catalano, G. Foti, E. Rimini, F. Eisen, and M.A. Nicolet *Solid-State Electron.* **21**, 485 (1978).

⁹J.L. Tandom, M.A. Nicolet, W.F. Tseng, F.H. Eisen, S.U. Campisano, G. Foti, and E. Rimini, *Appl. Phys. Lett.* **34**, 597 (1979).

¹⁰R. Tsu, J.E. Baglin, G.J. Lasher, and J.C. Tsang, *Appl. Phys. Lett.* **34**, 15 (1979).

¹¹P.A. Barnes, H.J. Leamy, J.M. Poate, S.D. Ferris, J.S. Williams, and G.K. Celler, *Appl. Phys. Lett.* **33**, 965 (1978).

¹²E.I. Shtyrkov, I.B. Khaibullin, M.M. Zaripov, M.F. Galjautdinov, and R.M. Bayazitov, *Sov. Phys. Semicond.* **9**, 1309 (1976).

¹³J.F. Ready, *Effects of High Power Laser Irradiation* (Academic, New York, 1971).

¹⁴P. Baeri, S.U. Campisano, G. Foti, and E. Rimini, *J. Appl. Phys.* **50**, 788 (1978).

¹⁵G.E.J. Eggermont, Y. Tamminga, and W.K. Hofken, in "Laser-Solid Interactions and Laser Processing", edited by S.D. Ferris, H.J. Leamy and J.M. Poate (AIP, New York, 1979); p. 321.

¹⁶L. Csepregi, J.W. Mayer, and T.W. Sigmon, *Appl. Phys. Lett.* **29**, 92 (1976).

¹⁷K. Gamo, T. Inada, J.W. Mayer, F.H. Eisen, and C.G. Rhodes, *Radiat. Eff.* **33**, 85 (1977).

¹⁸A. Gat, J.F. Gibbons, T.J. Magee, J. Peng, P. Williams, V. Deline, and C.A. Evans Jr., *Appl. Phys. Lett.* **33**, 389 (1978).

¹⁹J.C.C. Fan, J.P. Donnelly, C.O. Bozler, and R.L. Chapman, *Proc. 7th Intl. Symp. on GaAs and Related Compounds*, St. Louis, 1978 (unpublished).